Small-Size, Low-Weight, Single-Phase Inverter for Domestic Applications

Vijayakrishna Satyamsetti
Dept. of Engineering
University of Nicosia
Nicosia, Cyprus
vijayakrishna@ieee.org

Andreas Michaelides
Dept. of Engineering
University of Nicosia
Nicosia, Cyprus
michaelides.a@unic.ac.cy

Antonis Hadjiantonis
N.E.A Engineering Ltd.
Nicosia, Cyprus
antonis@neaeng.com

Anastasis C. Polycarpou
Dept. of Engineering
University of Nicosia
Nicosia, Cyprus
polycarpou.a@unic.ac.cy

Thanos Nicolaou
Ministry of Education
Nicosia, Cyprus
thanos.cy@cytanet.com.cy

***Abstract*—Rapid technological development in processor-controlled power electronics enables the employment of small transformers in their design, which leads to construction of lighter, smaller and, consequently, cheaper devices that are convenient to transport and store. The objective of this paper is to design a small, light, 12VDC to 240VAC, 50 Hz, ~500W inverter with a distortion factor of less than 2. This is performed with an efficient electronic circuit that forwards power through a high-frequency transformer. As a favorable output FFT spectrum is of major importance to the design of an inverter, Pulse Width Modulation (PWM) for the single-level unipolar inverter on the high voltage side, as well as conventional filtering techniques are employed. The design's performance is simulated in Matlab and its functional parameters are assessed with the overall prospect of building a prototype inverter at a later stage. The analysis presented herein reveals a 430W-capable inverter with dimensions 12×10×8cm, mass of 0.6Kg and total distortion factor of 1.4%, thus indicating fair prospects for the construction of such an inverter in the following months.**

Keywords—Inverter, solid-state transformer, distortion factor, unipolar pulse width modulation.

I. Introduction

Steady increase of domestic electric appliances requires an appropriate reliable power system of adequate quality. As AC power is not always and everywhere available, the necessity for portable AC power led to the development of the inverter. Inverters are thus widely being used for many decades. Probably the most common application known is the uninterrupted power supply (UPS) which provides information technology and other equipment with electricity during brief power outages. Inverters have also enjoyed wide range of applications in picnics and other outdoor recreational activities where they are connected to car batteries, thus enabling the supply of AC power to small refrigerators, television sets, lighting facilities and other low power home appliances. Early inverters were big and heavy, mainly due to the incorporated bulky transformer, and their output was a typical rectangular AC voltage of low power quality due to the high proportion of 3rd and 5th harmonics present. This had a negative influence on smooth motor rotation as it created additional heat and noise, reduced efficiency and, eventually, shorter equipment useful life.

The massive introduction of renewable energy sources to the power system (mainly wind generators and PV solar panels) resulted in decisive upgrading of the inverters' development for synchronization with and integration into the grid. A major significance of modern inverters is the employment of solid-state transformers (SST) [1] and processing of the output voltage via PWM [2]. The first leads to reduced size, mass and cost, whereas the latter to a 'true' sinusoidal output voltage which is advantageous for most AC devices, especially when utilizing timing circuits.

II. Concept

The construction of small size, low weight inverters is attributable to the combination of the considerably smaller solid-state transformers and sophisticated power electronics. The concept of using transformers with a much smaller cross section area relies on the increased rate of energy transfer in the core from the primary to the secondary side when operating at high frequencies [3]. The output of a unipolar DC to AC inverter provides three voltage levels:

- a positive DC voltage equal to the input DC voltage,
- a zero voltage, and
- a negative DC voltage, equal in magnitude to the input DC voltage.

The duration of and intervals between the positive and negative voltage pulses determine the overall average voltage at the inverter's output, as shown in Fig. 1.

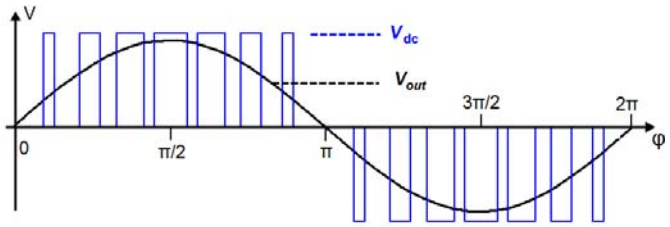

Fig. 1. Pulse Width Modulation (PWM) resulting to a sinusoidal output

978-1-5386-2910-9/18/$31.00©2018 IEEE

The current paper examines the possibility on this first stage to design the transformer for a high applied frequency. It also examines and analyzes the suitable electronic circuit, via Matlab simulation, in order to evaluate and optimize the inverter's performance.

The rest of the paper is organized as follows: Section III discusses the transformer design; section IV elaborates on the power electronics circuit of the design and section V presents and analyzes the results. Lastly, section VI provides valuable conclusions, especially with respect to the anticipated device construction to follow.

III. Transformer Design

The design of every power-processing electric machine starts, amongst others, from the magnetic material to be used. For the specific work herein, Magnetics Ferrite F 100 C was chosen as is deemed suitable to operate at high frequencies with low losses. Its magnetization *B-H* characteristic curve is presented in Fig. 2 [4]. From the figure, the optimal working point of the material is the point where the $B \cdot H$ product is maximum, just before entering saturation.

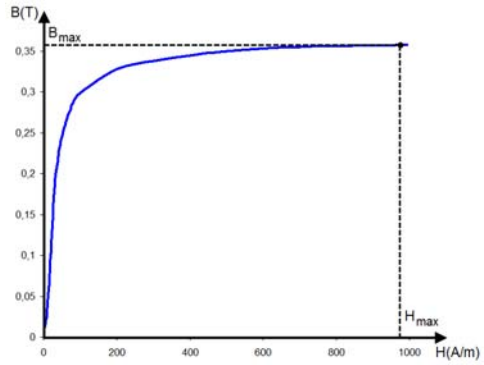

Fig. 2. Magnetization curve for Magnetics Ferrite F 100 C.

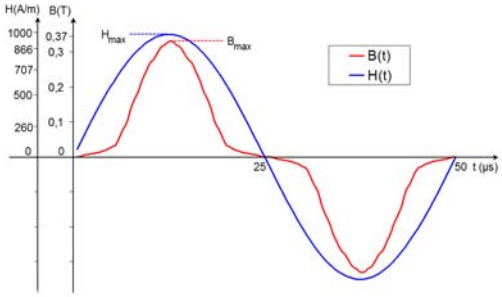

Fig. 3. Flux density and field strength as a function of time for one cycle.

The resulting appropriate *B(t)* and *H(t)* functions are presented in Fig. 3 over one cycle. These are established by the sinusoidal primary current and suggest that the energy density converted in the core in one cycle is the product of the two maxima divided by two (halving restores the round mean square values of the functions *B(t)* and *H(t)*):

$$e = \frac{B_{\max} \cdot H_{\max}}{2} \tag{1}$$

Assuming the hysteresis curve of the *B-H* characteristic of such a soft magnetic material to be very slim, this results in an insignificantly small phase shift between *H(t)* and *B(t)*, thus approximating the *B(t)* function by a sinusoidal function. For a specific core with cross section A and length l, the magnetization curve with optimal working point appears in terms of the magnetic flux Φ and the magneto motive force Θ, as shown in Fig. 4, where $\Phi = f(\Theta)$, as $B \cdot A = \Phi$ and $H \cdot l = \Theta$ (and l is the length and A the cross section area of the core).

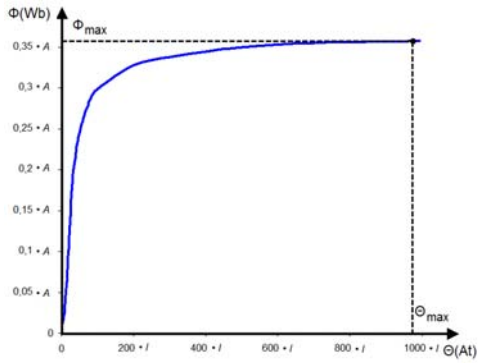

Fig. 4. Magnetic flux versus magnetomotive force.

Likewise, the energy converted in the core during one cycle can now be determined by:

$$E = \frac{\Phi_{\max} \cdot \Theta_{\max}}{2} \tag{2}$$

Multiplying the energy for a single cycle by the frequency results in the total energy per second, thus yielding the power (P) transferred through the core:

$$P = \frac{\Phi_{\max} \cdot \Theta_{\max} \cdot f}{2} \tag{3}$$

Aiming, as stated above, at a small-size transformer of high power conversion suggests the shell-type core design shown in Fig. 5. The shell-type core consists of two identical rectangular structural hollow sections shown clearly in Fig. 5a of square or rectangular cross section A shown in Fig. 5b.

The two sections are magnetically in parallel as the flux splits equally from the middle limb around the yokes to the two outer limbs [5]. Thus, the effective cross section of the shell-type transformer is twice the cross section A of one of the two sections whereas the effective transformer core length l is that of one section.

It is well known that increased power transfer is favored when cross section is big and core length is short. The shortest possible length, however, is determined by the required height of the windings on the middle limb, primary and secondary (shown in Fig. 5), in order to convert electrical to magnetic and magnetic to electrical power, respectively. An empirical geometric ratio only for small shell-type cores exists between the cross section and core length $k \cdot A = l$ where k is roughly about 500 per meter.

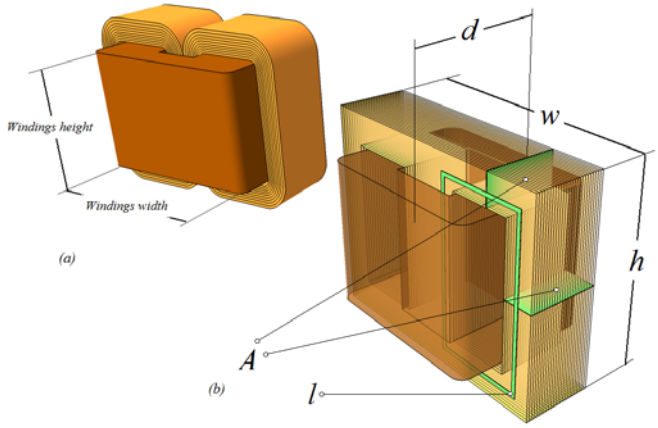

Fig. 5. Shell-type transformer.

The operational frequency of the transformer is determined by the maximum switching capability of the insulated gate bipolar transistors (IGBTs) used to invert the low input DC source to the high frequency AC signal to be further stepped up. The inverter designed here is anticipated to output a stable 20 kHz voltage in its future constructional stage. So, for a specific cross section A_i and the appropriate specific core length l_i at optimal working point (see Fig. 2), the power converted in a shell-type core, considering now the two structural hollow sections of Fig. 5a, is given by:

$$P_i = \Phi_{\max i} \cdot \Theta_{\max i} \cdot f \qquad (4)$$

Where $\Phi_{max\,i} = B_{max} \cdot A_i$ and $\Theta_{max\,i} = H_{max} \cdot l_1$, which reveals a clear connection between power rating and dimensions of the transformer's core.

TABLE. I. CALCULATIONS OF TRANSFORMER PARAMETERS

CSA (cm^2)	***VOLUME***			***M*** (Kg)	***P*** (W)
	Height (cm)	***Width*** (cm)	***Depth*** (cm)		
1,0	3,162	3,795	2,372	0,092	35,00
1,5	3,873	4,648	2,905	0,170	78,75
2,0	4,472	5,367	3,354	0,261	140,00
2,5	5,000	6,000	3,750	0,365	218,75
3,0	5,477	6,573	4,108	0,480	315,00
3,5	5,916	7,099	4,437	0,605	428,75
4,0	6,325	7,590	4,743	0,739	560,00
4,5	6,708	8,050	5,031	0,881	708,75
5,0	7,071	8,485	5,303	1,032	875,00

Table 1 presents the anticipated volume, mass and core power ratings of the transformer under a series of calculations for a range of different cross sections A and the appropriate core lengths l (obtained from the relation $k \cdot A = l$). The calculations assume optimal loading, that is B_{max} and H_{max} from Fig. 2, a frequency of 20 kHz and core material's density of 4.7 g/cm^3. To obtain the transformer mass, the core mass is multiplied by an empirical factor 1.3 accounting for the mass of the primary and secondary windings, connection terminals and taping material.

IV. Inverter Design

The design of the inverter is realized in four discrete stages, as depicted in Fig. 6. The actual circuit design is presented in Fig. 7.

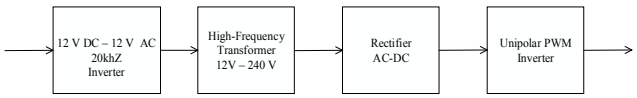

Fig. 6. The four stages of the design

Stage 1 converts the low-voltage 12VDC input to low voltage, high frequency, typical rectangular AC voltage ($\pm$ 12V) using four IGBT switches. The high frequency of this stage allows for the conversion of about 430W when forwarded through the primary side of the transformer, despite the transformer's small size.

In stage 2, this low voltage rectangular AC is fed to a high frequency insulation transformer to create a high voltage, high frequency rectangular AC.

In stage 3 this high voltage, high frequency signal is fed to a rectifier which converters it to a high voltage DC. The rectifier design, as seen in Fig. 7, requires increased consideration because of the high frequency nature of the signal. In usual bridge rectifiers, diodes have a long reverse recovery time of about 30 μs. Even fast recovery diodes (e.g., Schottky diodes), with a much shorter reverse recovery time of less than 1 μs are still not suitable for the present design as their reverse breakdown voltage is small, less than 100V, and the reverse current is relative high (about 10 mA). Choosing between the IGBT and Metal Oxide Field Effect Transistor (MOSFET) [7], both suitable for high frequencies in the range of 20 kHz, the latter prevails as it has a much smaller tailing current and hence, less turn-off losses. In addition, the MOSFET transistor has less on-state losses as its on-state resistance is smaller than that of the IGBT and the current in the present, 430W application, is relatively small (less than 5A).

However, concerns are expressed at this stage about the actual practical triggering of the rectifier because a pulse has to open transistors Q2 and Q3 by no means before the positive voltage appears at the transformer's secondary side. The pulse has then to be removed from transistors Q2 and Q3 shortly before the positive voltage changes to negative so that they already block when negative voltage appears. Likewise, pulses that trigger transistors Q1 and Q4 have to be removed with respect to the negative voltage at the transformer's secondary output be generated. This means that the processor has to be aware at any instance about the transformer's output state synchronizing the latter with the pulses.

A passive filter to reduce ripple and smoothening the signal and then in stage 4 converts the DC back to AC with four IGBTs employing unipolar PWM. Lastly, the output is filtered to remove the higher-order harmonics using a low-pass LC filter and the output is collected across a load resistor (not shown in Fig. 7).

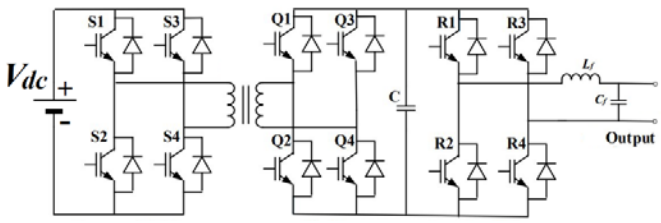

Fig. 7. Electronic circuit and solid state transformer constuting the inverter

For the constructed stage, the high frequency triggering of the inverter on the input side, as well as the rectifier, is intended to be realized with a programmable interface controller (PIC) driven by a 60 MHz oscillator. Furthermore, ripple rectification will be achieved by a 15 μF capacitor connected between the rectifier and the final inverter. The latter will perform unipolar pulse width modulation PWM to output a sinusoidal-like voltage. The interception of the zigzag function with the two sine functions determines the duration and interval of the positive and negative pulses at the output, as shown in Fig.8, and hence the shape of the average output signal. The modulating signals V_C and $-V_C$ oscillate with the intended output frequency of 50 Hz whereas the carrier zigzag function oscillates with 2 kHz resulting to an amplitude-modulation ratio and frequency-modulation ratio of m_a=1 and m_f=40, respectively. The high carrier frequency signal implies an equally fast triggering arrangement to be used as in the two previous stages.

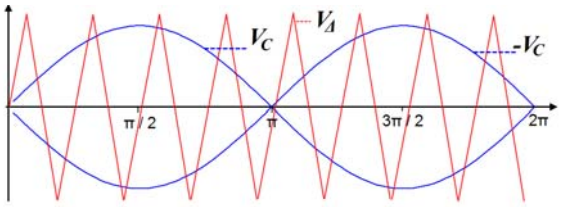

Fig. 8. Unipolar PWM. Modulating signal V_C Carrier signal V_Δ

Mere unipolar PWM, as presented in Fig. 1, outputs a sine-like voltage, which, however, is far from the ideal version depicted therein. Instead, the signal contains high harmonic modulations at unwanted frequencies and a high overall Total Harmonic Distortion (THD, or distortion factor). This is verified with simulation results depicted in Fig. 9 where an analysis of up to the 80th harmonic (4 KHz) revealed a THD of 52.14%. From this it is noted that, although PWM suppresses well most of odd-indexed harmonics (like the 3rd, 5th etc.), it allows for bands of unwanted odd-indexed frequencies (like the 35th to 45th and the 71st to 79th of Fig. 9) which contribute to a high THD. This distortion is further verified by the synthesis of the time signal of Fig. 10.

To mitigate this, a conventional, simple LC low-pass filter is deployed [8], as depicted in Fig. 7. The frequency characteristics of such a filter are presented in Fig. 11 where three different set of component values are examined: a critically damped case with L=20mH and C=1μF (red), an underdamped case with L=200mH and C=50μF (green) and an underdamped case with L=20mH and C=15μF (blue). The characteristics are for the case when the output is collected across a 100 Ohm resistor, which yields an output power close to the inverter's limit.

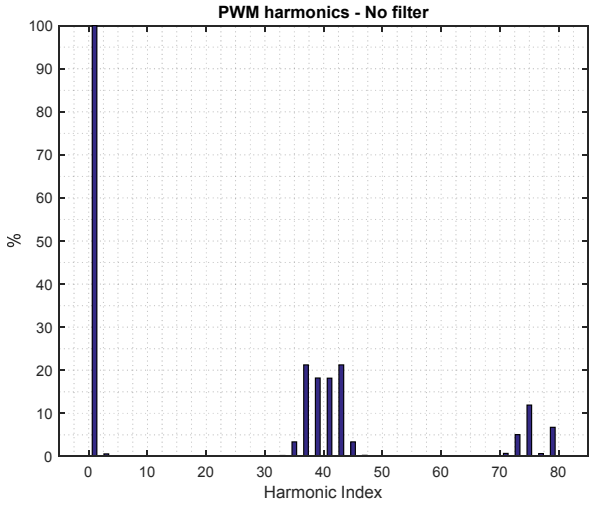

Fig. 9. FFT spectrum with out filter.

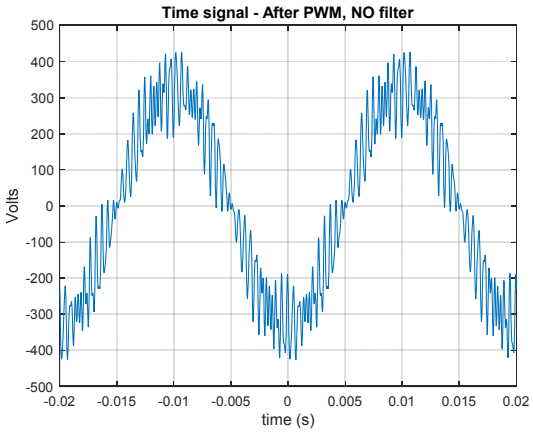

Fig. 10. Output waveform of inverter with out filter.

From Fig. 11, the critically damped case is not effective in clearing the higher frequencies and leads to an increased THD of 12.34%. The green, underdamped filter exhibits a small resonance but suppresses the higher frequencies very well and leads to a very small THD of 0.26%. Such a filter, however, is not realizable for the current design due to the high inductance (or capacitance, for that matter) it requires. The blue graph suppresses the higher frequencies considerably well (in between the previous two cases) and leads to a promising THD of 1.41% making it the desirable choice (a fine tradeoff between a realizable design and good performance).

It is worth noting that underdamped cases produce resonance: almost +4dB around the fundamental for the green filter, and +9dB (i.e. times $2\sqrt{2}$ in absolute terms) at $\omega_c = \frac{1}{\sqrt{LC}} = 1.83\frac{Krad}{s} = 290\text{Hz}$ for the blue filter. Although this is not wanted, it does not affect the harmonic distortion performance of the design, as the 3rd, 5th and 7th harmonics that

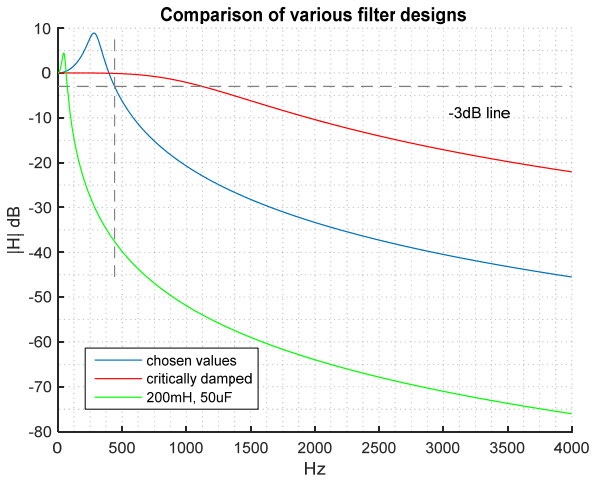

Fig. 11. Frequency response across the 100 Ohm resistor in the presence of the LC filter.

gain under these resonances were previously suppressed by the PWM process (see Fig. 9).This is verified by both theoretical analysis and Matlab simulation results.

Further, noting the Transfer Function of the inverter:

$$H(\omega) = \frac{1}{-LC\omega^2 + j\frac{L}{R_L}\omega + 1} \tag{4}$$

it is eminent that the load resistor R_L is an integral part of the frequency response. Specifically, as R_L increases, the resonance level of the underdamped cases is also expected to increase. Fortunately, the blue filter choice (L = 20mH and C = 15μF) produces the resonance at 290Hz, i.e. at around the almost non-existing 6th harmonic, so its effect is significantly contained only *around* it: on the 5th, just before it, and on the 7th just after it. For example, when a 100K Ohm resistor is used, which is translated to ~0.5W inverter output, we observe a gain of about a +10dB (times 3.16 in absolute terms) on the 5th and 7th harmonics (see Fig. 12), which, however, still yields an excellent THD of 1.71%.

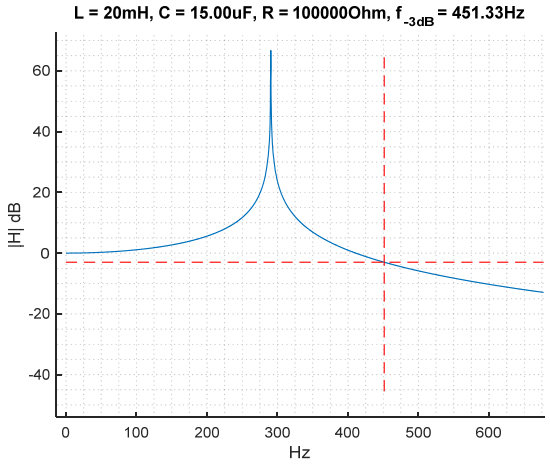

Fig. 12. High resonance for 100KOhm load

V. Simulation and Results

The design of the electronic circuit, as depicted in Fig. 7, is evaluated in Matlab's Simulink as this provides the possibility to operate the circuit under software simulation over many different parameter sets and diverse modes efficiently before the actual testing and construction. The simulations here progressed in steps of 50μs.

The transistors' declared parameters are with an internal resistance R_{on} = 1 mΩ, snubber resistance R_s =10 MΩ and snubber capacitance CS = ∞. The high frequency insulation transformer has a nominal power of 1 KVA at 2 KHz frequency (ratio follows below). The winding parameters are 0.002 pu and 0.08 pu and the magnetizing resistance (R_M) and inductances (L_M) are 500 pu. The rectifier uses ideal diodes with forward voltage V_f = 0.8 volts, internal resistance (R_{on}) and snubber resistance (R_s) of 500 Ω and snubber capacitance 250 nF.

The capacitor chosen to reduce ripple is 15 μF and the PWM IGBTs as per above. The values of L and C for the output Low-Pass filter, as well as its characteristics are as discussed above. As this output filter contains a series inductor, a voltage drop is anticipated which must be accounted for. To this end, in order to produce a ~230V AC, the high frequency insulation transformer ratio was set to raise the 12 Volts to 360 volts to counter-effect this drop.

Fig. 13 presents the output waveform collected across a load resistor of 100 Ω over two cycles. It is evident that, while the sinewave is not perfect, it appears to eliminate any significant unwanted frequency components. The peak-to-peak voltage is around 672.6 volts and an rms of 237.8 volts.

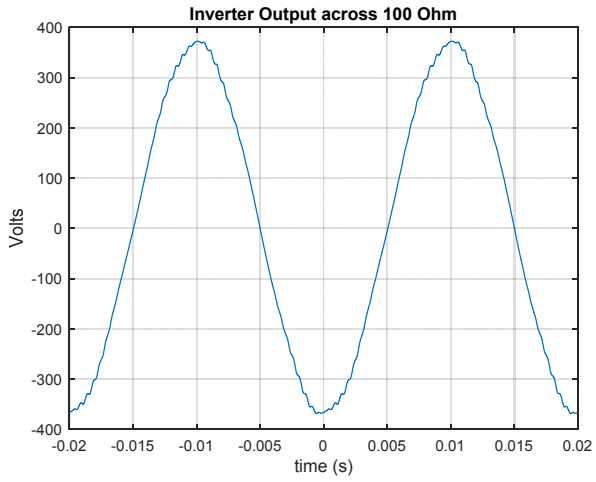

Fig. 13. Sinusoidal voltage at output over two complete cycles.

To quantify the distortion factor discussion, Fig. 14 presents the bar plot of the first 80 harmonics percentage contribution. Besides the 100% fundamental, the only other notable registered harmonic is the 3rd at 1.11% due to its amplification as it resides close to the resonance frequency of 290Hz.

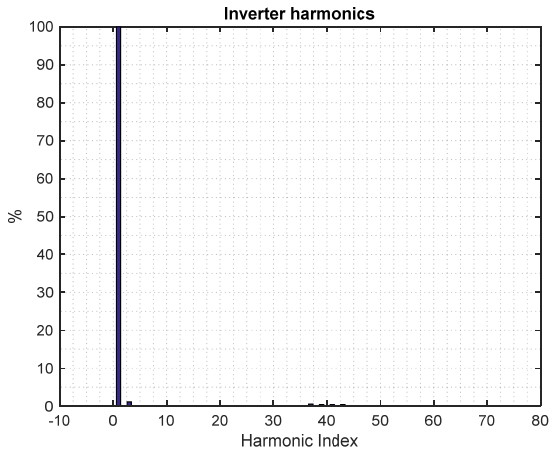

Fig. 14. FFT spectrum of output signal.

The overall final THD of the design is calculated at 1.4%, which is believed to be a promising result that enables the design to materialize. It has to be mentioned, however, that the almost ideal sinusoidal output and low distortion factor result from components being programmed with favorable parameters that might need more tweaking during the actual construction state.

VI. Conclusions

This paper presented the design of a single phase, 12VDC to 230VAC, 430W true sinewave inverter. The inverter, which employs an SST, has been calculated to be light and small-sized and, via Matlab simulation has been shown to be of low distortion factor and good output quality. The design, which is expected to be constructed at a later, final stage, is perused in two parts: the transformer design and the electronic circuitry processing the signal.

Conventional transformer design is usually being realized by provided equations [9] requiring many parameters which are often not readily available at initial stages. This leads to a process through lengthy inquiries and searches. In the present paper, however, an orthodox approach to energy conversion analysis has been followed. Easily obtainable characteristic values from the B-H magnetization curve (Fig. 2), that are assessed within simple Electrotechnical concepts focusing on the significance of the frequency aspect, provide a practical equation (equation 4) that includes only a basic core dimension, the cross section *A*, as shown in Fig.5b.

The targeted values are partly achieved as the volume resulting from the design is favorably small but the mass is considerably bigger as presented in Table 1. It is, however, anticipated that research focusing mainly on the magnetic materials is expected to yield improvement soon. Provisional voltage and current measurements of a usual shell-type cast iron core transformer of comparable size and mass show clearly the tendency that, for increased frequency, more power can be delivered.

The processing of the low 12V DC input power source up to the final ~230V rms, 50 Hz sinusoidal AC domestic supply signal is being realized by power electronics controlled by digital processing. The components of the circuit are declared in Matlab with almost ideal internal parameters. Apart from the filter on the output stage, the circuit design follows the conventional sequence of stages being applied for industrial power inverters that employ solid-state transformers. Hence, its Matlab simulation is straightforward and yields good results as expressed in the almost sinusoidal output voltage of Fig. 13 and the very low distortion factor of Fig. 14 with almost nonexistent harmonic modulations at unwanted frequencies.

The prospect of operating transistors with non-ideal parameters will not influence the qualitative functioning of the circuit significantly, as provisional measurements have shown.

Overall, the design of the transformer and the Matlab simulation results of the electronic circuit, which were complemented by provisional measurements, are well within anticipation and indicate reasonable prospects to consider engaging in the construction of the inverter.

References

[1] Boalong Liu, Yabing Zha, Tao Zhang, Shiming Chen, " Solid-state transformer application to grid connected photovoltaic inverters", International conference on smart grid and clean energy technologies (ICSGSE) , pp.248-251, October 2016.

[2] Jahangeer Soomro, T ayab D. Memon, M A. Shah " Design and analysis of a signel phase voltage source inverter using unipolar and bipolar pulse wodth modulation techniques", International conference on advances in Electrical Electronics Systems Engineering (ICAEES) , pp. 277-282, November 2016.

[3] H.R. Karampoorian, Gh.Papi , A. Vehedi, A. Zedehgol, " Optimum design of high-frequency transformer for compact and light weight switch mode power supplies (SMPS)" *IEEE GCC Confeence* pp.1-6 March 2016.

[4] Sunil M.Mutha, B.S.Umre, "Optimum utilization of Magnetization charecteristics of power capacity enhancement of the transformer and considerable saving in core cost*" IEEE Trans. on Magnetics*, vol. 52, No. 9, September 2016.

[5] Scott D. Sudhoff, " Transformer Design- Power Magnetic Devices: A Multi objective design approach", Wiley-IEEE Press eBook Chapters.

[6] Zhuoran Liu, Rujyang Yu, Tianxiang chen, Oingyun, Huang, Alex Q.Huang, "Real-time adaptive timing control of synchronous rectifiers in high-frequency GaN LLC converter", IEEE applied power electronics conferece and exposition, pp 2214-2220, USA, March 2018.

[7] Haihong Qin, Dan Wang, Ying Zhang, Dafeng Fu, Chaohui Zhao, " The charecteristic and switching strategies of SiC MOSFET assisted Si IGBT hybrid switch ", IEEE annual Industriual electronics society IECON China , November 2017.

[8] Manoj D. Patel, Rohit G. Ramteke, " L-C filter design implementation and comparative study with various PWM techniques for DCMLI", International conference on Energy systems and applications , pp. 347-352, India, November 2015.

[9] Jonas E. Huber, Johann W. Kolar, "Solid state transformers on the origin and evolution of key concepts*", IEEE Industrial Electronics Magazine*, pp. 19-28, September 2016.